2026 JULY 19–22 VANCOUVER, BC
JOINT AAPM | COMP MEETING

Optimizing X-ray Beam Quality for Low-Dose Upright Cone-Beam Breast CT using Advanced Image Reconstruction Algorithm

Hsin Wu Tseng, PhD; Jing-Tzyh Alan Chiang, MD PhD; Srinivasan Vedantham, PhD
The University of Arizona, Tucson, AZ

ABSTRACT

Purpose: To determine the optimal X-ray beam quality by varying the copper (Cu) filter thickness for upright cone-beam breast CT (CBBCT) to achieve a mean glandular dose (MGD) of approximately 4.5 mGy, which is suitable for breast cancer screening, while maintaining microcalcification visibility.

Methods: Five acquisition protocols were evaluated using a breast phantom containing 0.24–0.32 mm diameter spherical calcium carbonate microcalcifications. The following parameters were fixed: 60 kV, 50 mA, 20 ms pulse width, 210° angular range. Cu filter thickness was varied (0.05–0.25 mm) with the number of projection views adjusted to maintain MGD of approximately 4.5 mGy. All datasets reconstructed were using FRIST. Two readers independently evaluated microcalcification cluster visibility.

Results: The 0.15 mm Cu filtration and 90-view protocol (MGD 4.52 mGy) provided optimal 0.24 mm calcification visibility using FRIST reconstruction. Protocols with extreme undersampling (62 and 36 views) exhibited streak artifacts. Thicker Cu filtration showed reduced calcification visibility due to increased noise.

Conclusion: For low-dose upright CBBCT, 0.15 mm Cu with 90 views represents the optimal balance between beam quality and angular sampling, enabling reliable microcalcification detection at MGD of 4.5 mGy using compressed sensing-based FRIST reconstruction.

CONTACT

Srinivasan Vedantham, PhD
Department of Radiology & Imaging Sciences
The University of Arizona
Telephone: +1 520-626-6641
Email: svedantham@arizona.edu

INTRODUCTION

Digital Mammography (DM) and Digital Breast Tomosynthesis (DBT) are current standard-of-care modalities for breast cancer screening. However, tissue superposition in DM and slice separation artifacts in DBT remain as limitations.

Dedicated cone-beam breast CT (CBBCT) provides fully three-dimensional (3D), compression-free imaging of the breast with isotropic voxel resolution and eliminates tissue superposition. The upright geometry improves patient comfort by eliminating the challenges with prone positioning.

X-ray beam quality — primarily determined by filtration — governs the tradeoff between photon fluence per projection and beam penetration. At fixed MGD, thinner Cu filtration provides higher X-ray fluence per projection but requires extreme angular undersampling. Thicker filtration reduces X-ray fluence per projection but allows for improved angular sampling.

The compressed sensing-based Fast, total variation-Regularized, Iterative, Statistical reconstruction Technique (FRIST) is optimized for sparse-view acquisitions and enables dose reduction while preserving image quality [1-3].

METHODS AND MATERIALS

Pictures of the upright dedicated breast CT system are shown in Fig 1.

Breast phantom: The breast phantom is semi-ellipsoidal in shape with 20% homogenous fibroglandular composition and dimensions approximating an average uncompressed breast. It contains pentagon-shaped clusters of spherical calcium carbonate ($CaCO_3$) microcalcifications: 0.24, 0.27, 0.29, 0.32 mm diameters. There are six calcifications per cluster (1 center + 5 vertices). The success criterion is visibility of ≥4/6 spheres per cluster (≧67%).

Reconstruction: Reconstruction was performed using Fast, total variation-Regularized, Iterative, Statistical Technique (FRIST) [1-3] to 0.1 mm isotropic voxels followed by rebinning to 0.2 mm. The FRIST hyperparameters are: $\alpha=2\times10^{-3}$, $\beta=1$, 130 iterations.

Reader Evaluation: Two readers (diagnostic medical physicist and breast imaging radiologist) performed independent blinded evaluation.

Table 1. Summary of acquisition protocols and mean glandular dose (MGD) for an average breast. The following parameters were fixed: 60 kV, 50 mA tube current, 20 ms X-ray pulse-width, 210° angular range.

Protocol	Cu Filter	Views	MGD (mGy)
(a)	0.25 mm	210	4.27
(b)	0.20 mm	126	4.53
(c)	0.15 mm	90	4.52
(d)	0.10 mm	62	4.54
(e)	0.05 mm	36	4.60

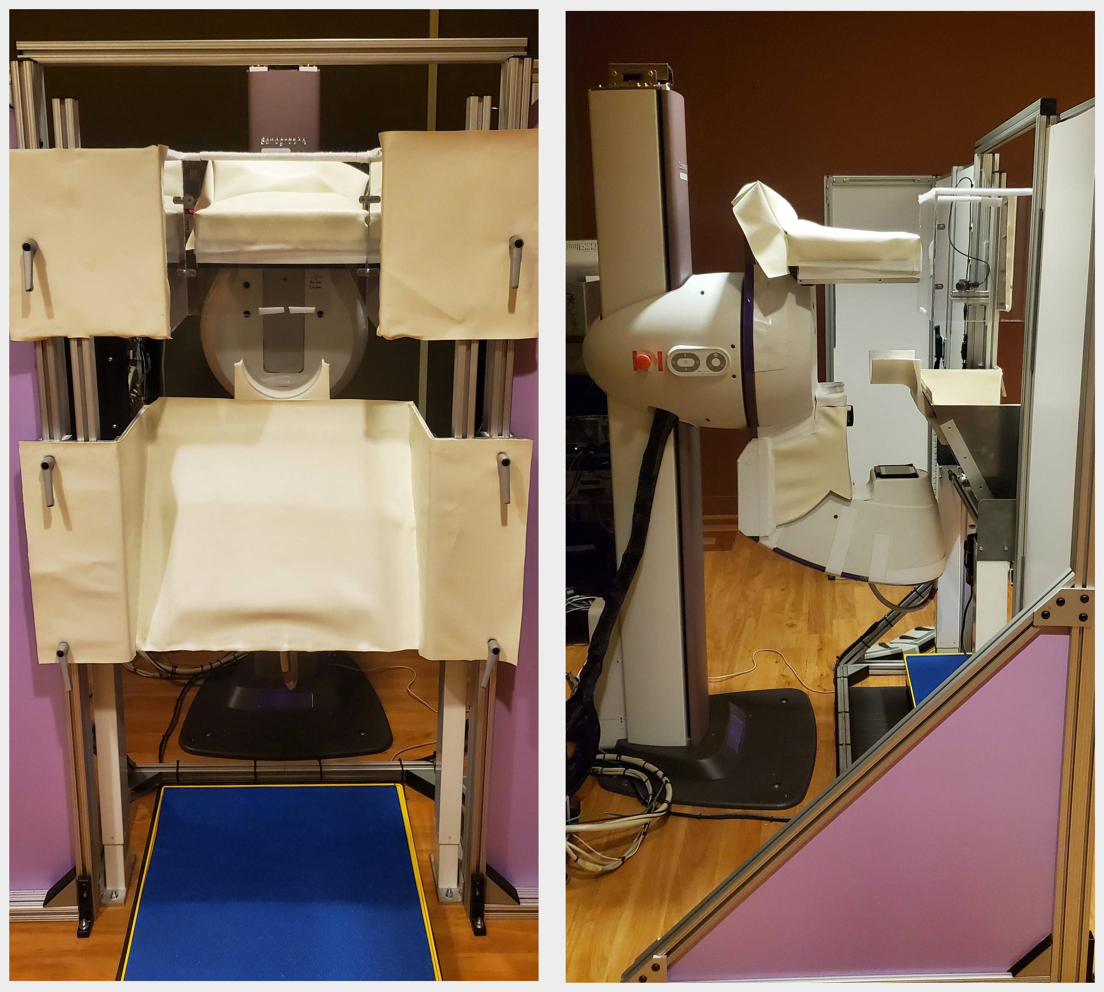

Figure 1. Pictures of the upright cone-beam breast CT system. Left: front (patient) view; Right: side view.

RESULTS

The number of spheres averaged across the two readers for each cluster is summarized in Table 2.

The key finding is that 0.15 mm Cu filtration and 90 projection views that result in 4.5 mGy MGD maximized visibility of microcalcifications and allowed visualizing 0.24 mm calcification cluster.

Thick section (2 mm from 10 slices) maximum intensity projection (MIP) images are shown in Figure 2.

Table 2. Number of visible microcalcifications per cluster (averaged from 2 readers).

Cu Filter	Views	MGD (mGy)	0.32 mm	0.29 mm	0.27 mm	0.24 mm ★
0.25 mm (a)	210	4.27	6	5	3	1.5
0.20 mm (b)	126	4.53	6	3	2	1
0.15 mm (c) ★	**90**	**4.52**	**6**	**5.5**	**6**	**4.5 ✓**
0.10 mm (d)	62	4.54	—	—	—	Streak ✗
0.05 mm (e)	36	4.60	—	—	—	Streak ✗

★ indicates optimal protocol. ✓ indicates detection criterion of ≥4/6 spheres in each cluster was met. ✗ indicates that detection criterion failed. — indicates that there were substantial streak artifacts, which precluded scoring.

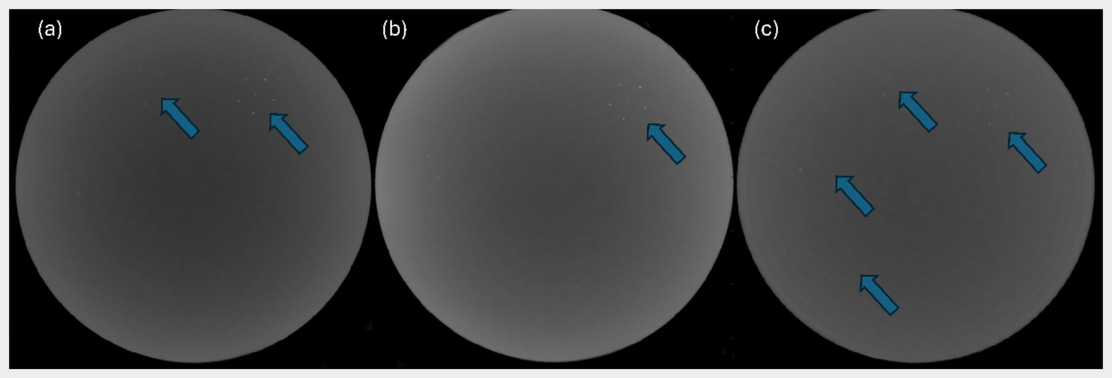

(a) 0.25 mm Cu, 210 views, MGD: 4.27 mGy
(b) 0.20 mm Cu, 126 views, MGD: 4.53 mGy
(c) 0.15 mm Cu, 90 views, MGD: 4.52 mGy

Figure 2. Thick section (2 mm) Maximum Intensity Projection (MIP) images from 10 slices reconstructed using FRIST. Blue arrows indicate microcalcification clusters that met the detection criterion (≥4/6 spheres in each cluster was visualized). In (a) and (b), detection criterion for 0.27 and 0.24 mm was not satisfied. In (c), 4.5 (average of 2 readers) of the 6 spheres forming the 0.24 mm cluster was visualized.

DISCUSSION

Why does 0.15 mm Cu represent the optimum?

The tradeoff between Cu filter thickness and number of projection views is governed by two competing factors:

Thinner Cu filtration (0.05–0.10 mm): Allows greater X-ray fluence per projection (lower quantum noise) but requires extreme angular undersampling (36–62 views) to maintain a MGD of approximately 4.5 mGy. At these view counts, streak artifacts are severe and exceed FRIST's iterative correction capacity, rendering calcification visualization unreliable.

Thicker Cu filtration (0.20–0.25 mm): Permits increased number of projection views (126–210) due to reduced MGD per view. However, the increased beam hardening reduces X-ray fluence per projection, increasing quantum noise per projection and degrading microcalcification conspicuity despite improved angular sampling.

*0.15 mm Cu at 90 views***:** Provides sufficient angular sampling for FRIST to effectively suppress undersampling artifacts, while maintaining adequate photon fluence per projection to achieve acceptable signal-to-noise ratio for 0.24 mm calcification detection.

Role of FRIST: FRIST enforces a hard data consistency constraint ($\|Ax-b\|_2 \le \varepsilon$) via iterative correction between TV-minimization steps, driving the reconstruction towards the measured projections while suppressing streak artifacts.

CONCLUSIONS

- At MGD of 4.5 mGy and using compressed sensing-based FRIST reconstruction, 0.15 mm Cu filtration with 90 projection views is the optimal acquisition protocol for low-dose upright CBBCT.
- For the optimal protocol, FRIST enables reliable detection of 4.5/6 individual spheres of 0.24 mm diameter forming the calcification cluster — a clinically relevant size for early breast cancer detection — at screening-compatible dose.
- The results establish a standardized low-dose protocol to support investigating upright breast CT as a potential screening modality.

REFERENCES

1. Tseng HW, Karellas A, Vedantham S. Cone-beam breast computed tomography using ultra-fast image reconstruction with constrained, total-variation minimization for suppression of artifacts. Phys Med. 2020;73:117–124. doi:10.1016/j.ejmp.2020.04.020
2. Tseng HW, Karellas A, Vedantham S. Sparse-view, short-scan, dedicated cone-beam breast computed tomography: image quality assessment. Biomed Phys Eng Express. 2020;6(6). doi:10.1088/2057-1976/abb834
3. Tseng HW, Karellas A, Vedantham S. Cone-beam breast CT using an offset detector: effect of detector offset and image reconstruction algorithm. Phys Med Biol. 2022;67(8). doi:10.1088/1361-6560/ac5fe1

Acknowledgments: Supported in part by the American Cancer Society (ACS) grant IRG-18-161-40 and in part by the National Cancer Institute (NCI) of the National Institutes of Health (NIH) grant R01 CA241709. The contents are solely the responsibility of the authors and do not necessarily reflect the official views of the ACS, NCI, or the NIH.